ACS OMEGA

Open Access

http://pubs.acs.org/journal/acsodf

Article

Miniaturization of Sub 6 GHZ Band 5G Monopole Antenna with Manganese Assisted $CoFe_2O_4$ Nano Self-Assembly Magneto-Dielectric Coating

Venkatesh Dayanidhi,* Thiyagarajan Krishnan, and Thangaraju Dheivasigamani

Cite This: *ACS Omega* 2025, 10, 26041−26051

Read Online

ACCESS | Metrics & More | Article Recommendations

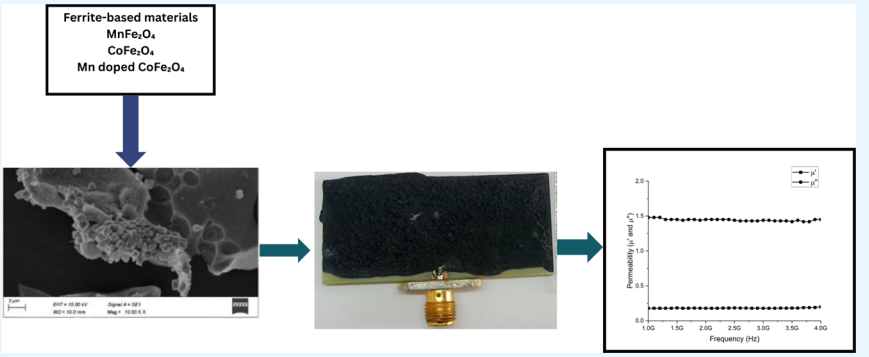

ABSTRACT: This paper proposes a miniaturized monopole antenna for sub-6 GHz 5G mobile applications by integrating a magneto-dielectric superstrate. The Magneto dielectric material is composed of manganese-assisted $CoFe_2O_4$ ferrite-based nanoself-assembly materials. The Gel Matrix method is utilized to synthesize $MnFe_2O_4$, $CoFe_2O_4$, and Mn-doped $CoFe_2O_4$ magneto-dielectric ferrite nanoparticles. Structural and morphological analysis of the synthesized particles is conducted using X-ray diffraction (XRD) and scanning electron microscopy (SEM). The magneto-dielectric (MDL) coating over the antenna is done by mixing the ferrite powders with polyvinylidene fluoride (PVDF) polymer. The effects of the magneto dielectric layer on the monopole antenna's performance are assessed in terms of return loss, radiation pattern, and impedance bandwidth using a vector network analyzer and an Anechoic Chamber. A significant improvement in the impedance bandwidth (400 MHz) is observed for the Mn-doped $CoFe_2O_4$−PVDF coating, achieving a bandwidth of 3.00 to 3.4 GHz. The antenna exhibits miniaturization with a resonance frequency shift to 3.2 GHz, achieving a peak gain of 2.6 dBi. The results demonstrate that the Mn-doped $CoFe_2O_4$−PVDF superstrate effectively supports antenna miniaturization for the sub-6 GHz frequency bands, such as n77 and n78, used in 5G applications.

1. INTRODUCTION

The rapid evolution of wireless communication technologies over the past decade has ushered in a new era of connectivity, driven largely by the advancements in 5G networks. 5G, the fifth generation of mobile communication, promises a paradigm shift in communication systems, offering enhanced data speeds, ultrareliable low-latency connectivity, and massive network capacity. With the increasing demand for mobile devices and the explosion of data traffic, the design of antennas capable of supporting these technologies has become a critical area of research and development.[1−4]

One of the key frequency bands utilized for 5G networks is the sub-6 GHz spectrum, which is essential for ensuring broad coverage and high capacity in mobile communication systems. In particular, the n77 and n78 bands, falling within the 3.3 to 3.8 GHz range, are crucial for 5G deployments in many regions globally, including Europe, Asia, and parts of North America. These bands are especially significant for mobile devices like smartphones, tablets, and other connected devices, which require compact, efficient, and high-performance antennas to meet the stringent requirements of 5G networks.[5−7]

The challenge in antenna design lies in the need to balance performance with size constraints, particularly for mobile devices where space is limited. As a result, antenna miniaturization techniques have gained considerable attention. Conventional methods for antenna miniaturization often involve altering the geometry or topological structure of the antenna, such as reducing the length of the radiator or

Received: March 27, 2025
Revised: May 31, 2025
Accepted: June 6, 2025
Published: June 11, 2025

employing fractal designs. While effective, these methods may lead to a reduction in bandwidth, efficiency, or radiation characteristics.[8−10]

To overcome these limitations, researchers have turned to alternative materials that exhibit both dielectric and magnetic properties, known as magneto-dielectric materials. These materials offer the potential to miniaturize antennas while improving their performance, particularly in terms of impedance matching, bandwidth, and radiation efficiency. Magneto-dielectric materials have the advantage of enhancing the effective permittivity and permeability of the antenna's substrate or superstrate, which can significantly affect the antenna's size and resonance characteristics. This is particularly useful for applications in the sub-6 GHz frequency range for 5G communications.[11,12]

Among the various magneto-dielectric materials, ferrite-based compounds have proven to be particularly effective. Ferrites, especially those doped with elements like manganese (Mn) or cobalt (Co), exhibit strong magnetic properties and can be engineered to display tailored dielectric and magnetic characteristics.[13] These materials, when incorporated as superstrates in antenna designs, can lead to significant miniaturization of the antenna without compromising its performance. The doping of manganese into cobalt ferrite ($CoFe_2O_4$) results in a change in the material's magnetic and dielectric properties, shifting the ferromagnetic resonance (FMR) frequency, which can be exploited for the miniaturization of antennas. Moreover, $CoFe_2O_4$ and $MnFe_2O_4$ materials also offer excellent stability and high permeability at microwave frequencies, making them ideal candidates for 5G applications.[14,15] The hollow carbon nanocages with $CoFe_2Se_4$ quantum dots (HCNsQCoFe_2Se_4-QDs), Self-confined method to create hierarchical Fe−Co@TiO_2 microrods, hollow CuS⊕CoS_2 nanoboxes with double shells, Co/N-doped porous carbon (Co/NPC) composites were also used as microwave absorbers.[16−19]

This study explores the integration of Mn-doped $CoFe_2O_4$ and $CoFe_2O_4$ as magneto-dielectric superstrates for monopole antennas operating in the sub-6 GHz frequency range for 5G mobile device applications. The main objective is to investigate the potential of these materials to enhance antenna performance through miniaturization, improved impedance matching, and extended bandwidth. Specifically, the research focuses on the synthesis and characterization of Mn-doped $CoFe_2O_4$ and $CoFe_2O_4$ nanostructures, their integration into the antenna design, and the resulting performance improvements in terms of resonance frequency, return loss, gain, and radiation pattern.[14,15]

By synthesizing ferrite nanoparticles using the Gel Matrix method, and coating them onto the monopole antenna, this work seeks to demonstrate the impact of these magneto-dielectric materials in the miniaturization of 5G antennas, specifically targeting the n77 and n78 bands. The combination of these advanced materials with a simple polymer-based matrix offers an innovative approach for enhancing the antenna's efficiency while addressing the space limitations typical in mobile devices.[14,20,21] The remainder of this paper is structured as follows: Section 2 outlines the synthesis and characterization of the magneto-dielectric materials, Section 3 presents the design and characterization of the monopole antenna with and without the magneto-dielectric superstrate, and Section 4 discusses the conclusions drawn from the study.

2. MAGNETO-DIELECTRIC NANOSTRUCTURE SYNTHESIS

Electromagnetic waves consist of both dielectric and magnetic components, which require substrates or superstrates with suitable properties for effective transmission. For antenna applications, particularly at microwave frequencies ranging from 500 MHz to several GHz, materials must exhibit both high dielectric and magnetic properties. However, many materials with high magnetic permeability exhibit paramagnetic behavior at these frequencies due to the inability of magnetic domains to align with the rapid phase reversals of the electromagnetic field. The frequency at which this transition occurs is known as the ferromagnetic resonance frequency (Snoke limit), beyond which magnetic losses dominate.[22,23]

For effective antenna performance, a magneto-dielectric material should have constant permittivity and permeability values greater than one across the required frequency range, along with a low loss tangent. As the frequency increases, the permeability of materials tends to decrease, and magnetic losses increase due to residual magnetic flux that remains after the external magnetic field is applied. At higher frequencies, the magnetic domains cannot align quickly enough with the rapidly changing external field, resulting in a decrease in magnetic properties.[24−26]

To address these challenges, magneto-crystalline anisotropy plays a crucial role. This property depends on the stoichiometry, crystal structure, and morphology of the material, which are influenced by the synthesis method. Materials with homogeneous magnetic permeability require precise control over these factors. Among various synthesis methods, the self-propagating high-temperature synthesis (SHS) technique is favored for its high yield, phase purity, and the ability to form compounds at low temperatures with fine grain sizes. For the synthesis of magneto-dielectric nanostructures like $CoFe_2O_4$, Mn-doped $CoFe_2O_4$, and $MnFe_2O_4$, the Gel Matrix method was employed. This method allows for precise control over the stoichiometry and morphology of the ferrite materials, ensuring homogeneous magnetic properties.[27−29]

The synthesis procedure begins with the preparation of the precursor solution, where Cobalt(II) nitrate hexahydrate ($Co(NO_3)_2{\cdot}6H_2O$) and Ferric nitrate nonahydrate ($Fe(NO_3)_3{\cdot}9H_2O$) are dissolved separately in two beakers, each containing 25 mL of water. After the complete dissolution of the salts, the solutions are mixed together, and citric acid monohydrate ($C_6H_8O_7{\cdot}H_2O$) is added as a chelating agent (3 mmol), followed by stirring for 5 min. To promote polymerization of the metal-citrate complexes, ethylene glycol ($C_2H_6O_2$) is introduced into the solution.[30,31]

Next, the solution is heated to 80 °C to remove excess liquid and induce polymerization, resulting in the formation of a gel. The dried gel flakes are then prefired at 250 °C in a muffle furnace, followed by annealing at 550 °C for approximately 1 h to achieve the desired crystalline structure. Once cooled to room temperature, the resulting powder consists of $CoFe_2O_4$, Mn-doped $CoFe_2O_4$, and $MnFe_2O_4$ magneto-dielectric materials, ready for use as coatings on fabricated antennas, such as the 3.4 GHz antenna in this study. This synthesis method allows for precise control over the material properties, ensuring the resultant nanostructures exhibit the necessary magnetic and dielectric characteristics for optimal antenna performance. The resultant powders were characterized using XRD and SEM

https://doi.org/10.1021/acsomega.5c02680
ACS Omega 2025, 10, 26041−26051

to assess the phase purity, crystal structure, and surface morphology.[32−34]

3. STRUCTURAL AND ELECTROMAGNETIC CHARACTERIZATION

3.1. Structural Characterization. The structural characterization of the synthesized materials—$CoFe_2O_4$, Mn-doped $CoFe_2O_4$, and $MnFe_2O_4$—was conducted using XRD, as presented in Figure 1. The XRD patterns of all three materials

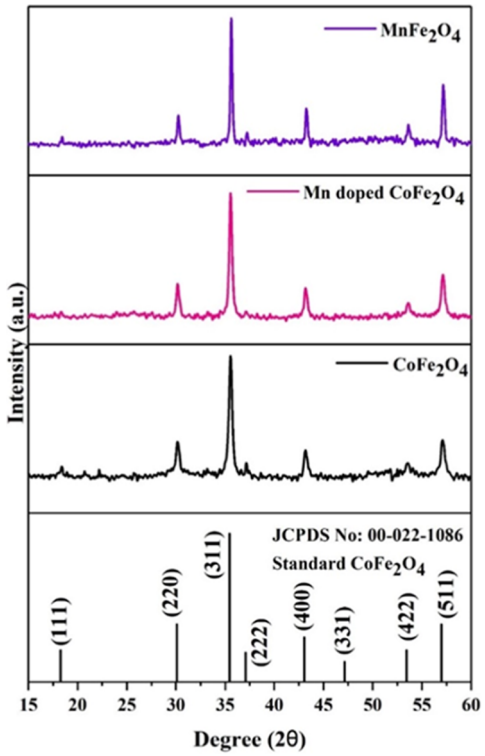

Figure 1. X-ray diffraction pattern of $CoFe_2O_4$, Mn doped $CoFe_2O_4$ and $MnFe_2O_4$ particles.

reveal that they exhibit a cubic crystal structure, specifically aligning with the $Fd\bar{3}m$ space group (JCPDS No.: 00-022-1086). This phase identity confirms that the materials are of high crystalline quality, and importantly, no impurity peaks were observed, indicating phase purity. The absence of additional peaks confirms that the synthesis method employed does not introduce any unintended phases, ensuring the homogeneity of the final product.[33,34]

Notably, the $MnFe_2O_4$ samples demonstrate a shift in the reflection peaks toward higher angles compared to $CoFe_2O_4$. This shift is attributed to the substitution of Fe^{3+} ions by Mn^{2+} or Mn^{3+} ions in the crystal lattice, which alters the lattice parameters. The larger ionic radius of Mn compared to Fe results in a contraction of the lattice, thus causing the reflection peaks to shift to higher angles. This shift serves as a clear indication of the influence of Mn doping on the crystal structure, affecting both the lattice spacing and the overall crystallographic characteristics of the material.[34−36]

In addition to the XRD analysis, SEM was employed to further investigate the morphology of the ferrite particles, as shown in Figure 2. The SEM images reveal that the $CoFe_2O_4$ particles exhibit a unique self-assembled, wasp-nest-like structure. This characteristic morphology suggests a well-

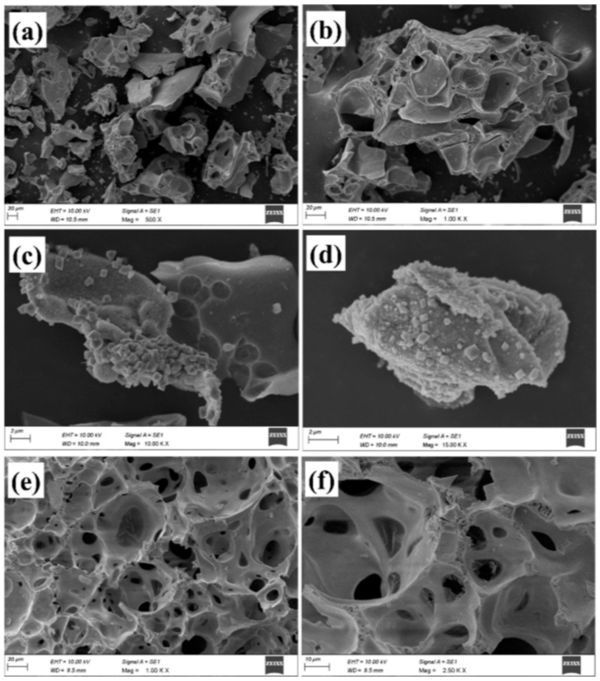

Figure 2. FESEM images of $CoFe_2O_4$ (a,b), Mn doped $CoFe_2O_4$ (c,d) and $MnFe_2O_4$ (e,f) partcles.

organized assembly of particles, which is essential for the material's performance in magneto-dielectric applications. On the other hand, Mn doping leads to a more compact, diamond-shaped morphology for the Mn-doped $CoFe_2O_4$ particles. This change in shape and structure indicates that the Mn ions play a role in controlling the particle assembly, possibly enhancing the material's structural integrity and its response to external electromagnetic fields.[33,37,38] The $MnFe_2O_4$ particles display a reduced thickness in the surface assembly compared to the $CoFe_2O_4$ and Mn-doped $CoFe_2O_4$ samples, suggesting a more periodic dispersion of the particles. This periodic arrangement could be beneficial for enhancing the magnetic and dielectric properties, as the regular spacing between particles may contribute to more uniform interactions with external fields, promoting improved performance in antenna and sensor applications.[39,40]

Overall, the XRD and SEM analyses provide crucial insights into the phase purity, crystal structure, and morphological characteristics of the synthesized materials, confirming the successful incorporation of Mn into the ferrite matrix and highlighting the changes in structural properties that result from the doping process. These structural features are critical to the materials' electromagnetic properties and their suitability for use in advanced magneto-dielectric applications, particularly in antenna technologies.

3.2. X-ray Photoelectron Spectroscopy. The elemental composition and corresponding oxidation states of the synthesized $CoFe_2O_4$ and Mn doped $CoFe_2O_4$ nanoparticles were thoroughly investigated using XPS analysis. Figures 3 and 4 presents the core-level XPS spectra for Co 2p, Fe 2p, and O 1s in $CoFe_2O_4$ and Co 2p, Fe 2p, Mn 2p and O 1s in Mn doped $CoFe_2O_4$ nanoparticles, offering valuable insight into the chemical states of cobalt, iron, manganese and oxygen within the samples. In the Co 2p spectrum (Figures 3a and 4a), two prominent peaks are observed at binding energies of approximately 780 and 796 eV. These are assigned to Co $2p_{3/2}$

https://doi.org/10.1021/acsomega.5c02680
ACS Omega 2025, 10, 26041−26051

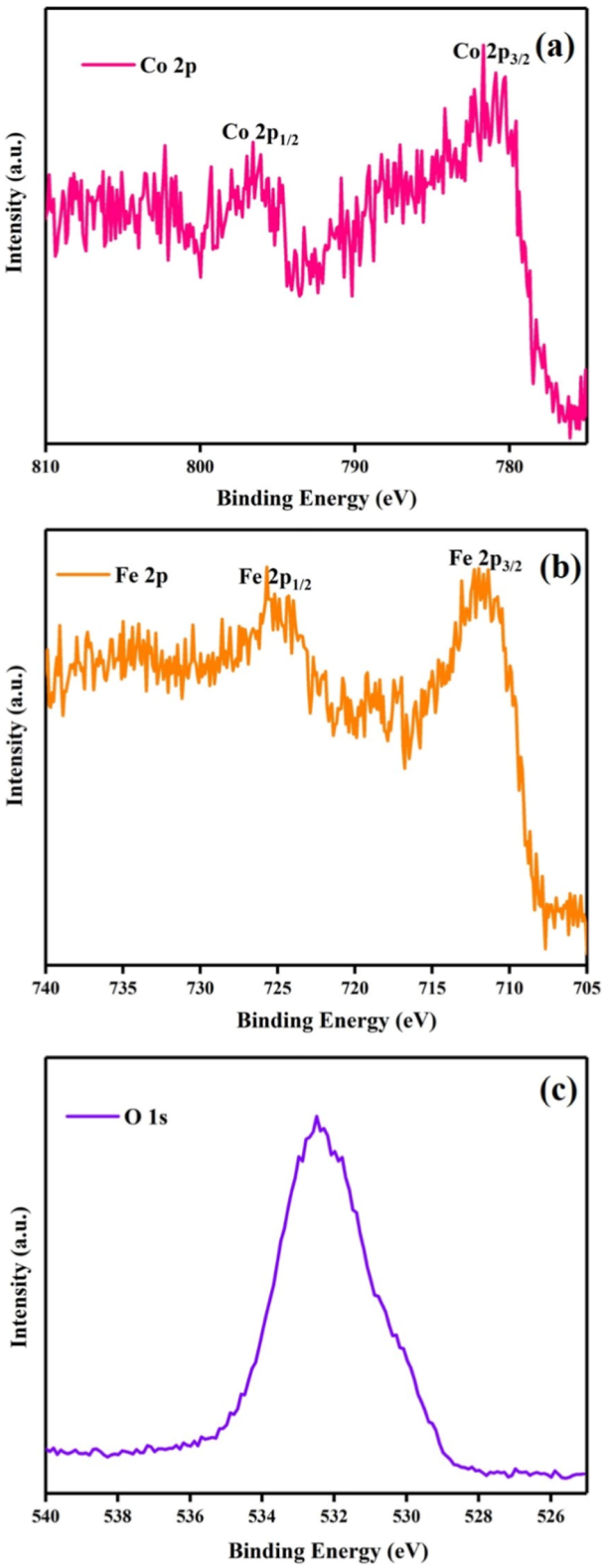

Figure 3. XPS spectra of Co 2p (a), Fe 2p (b) and O 1s (c) for pure $CoFe_2O_4$.

and Co $2p_{1/2}$, respectively, which are characteristic of Co^{2+} species, confirming the presence of divalent cobalt in the material. Similarly, the Fe 2p spectrum (Figures 1b and 2b) displays distinct peaks near 708 and 723 eV, corresponding to Fe $2p_{3/2}$ and Fe $2p_{1/2}$, respectively. These binding energies are indicative of Fe^{3+} oxidation state, as they match well with reported values for ferric iron. The absence of peaks associated with Fe^{2+} further supports that the iron predominantly exists in the Fe^{3+} state in the prepared samples. The O 1s spectra of both $CoFe_2O_4$ (Figure 1c) and Mn doped $CoFe_2O_4$ (Figure 4d) materials reveal two main peaks centered around 530 and 532 eV, respectively. The binding energy peak at ∼530 eV is attributed to lattice oxygen involved in metal−oxygen bonding, confirming the formation of metal oxides. Meanwhile, the energy peak at ∼532 eV in $CoFe_2O_4$ material is associated with adsorbed oxygen species or surface-adsorbed water molecules, which are commonly present due to atmospheric exposure. Figure 4c depicts the Mn 2p spectra of Mn doped $CoFe_2O_4$ material with peaks at binding energies of 653 and 641 eV correspond to the Mn $2p_{1/2}$ and Mn $2p_{3/2}$ spin−orbit components, respectively. This confirms the presence of Mn^{3+} in Mn doped $CoFe_2O_4$. These findings collectively confirm the successful incorporation of Manganese in pure $CoFe_2O_4$ synthesized material.

3.3. Electromagnetic Characterization. To characterize the magneto-dielectric substrates, the complex *S*-parameters were measured using a vector network analyzer (VNA). Prior to testing, the synthesized material was processed into pellets with dimensions of 2.2 mm × 1.01 mm. For the measurement of the material's electromagnetic properties, the transmission/reflection-based non-resonant approach was chosen, as it allows for the simultaneous measurement of permittivity and permeability over a broad frequency range. This approach is well-suited for characterizing magneto-dielectric materials as it can capture both dielectric and magnetic responses across a wide bandwidth.[41,42]

The *S*-parameters were analyzed to extract the complex permittivity and permeability values. While other algorithms may assume a permeability value of one and derive the electromagnetic characteristics based on this assumption, the Nicolson-Ross-Weir (NRW) technique is preferred for magnetic materials, as it allows for the accurate extraction of both permittivity and permeability.[43,44]

The reflection coefficient (Γ) is calculated using the eq 1

$$\Gamma = K \pm \sqrt{K^2 - 1} \tag{1}$$

where K is given by equation by the eq 2

$$K = \frac{(S_{11}^2 - S_{21}^2) + 1}{2S_{11}} \tag{2}$$

The transmission coefficient (T) is calculated by the eq 3

$$T = \frac{(S_{11} + S_{21}) - \Gamma}{1 - (S_{11} - S_{21})\Gamma} \tag{3}$$

The permittivity and permeability are calculated by the eqs 4 and 5

$$\mu_r = \frac{1 + \Gamma}{(1 - \Gamma)\Lambda\sqrt{\frac{1}{\lambda_0^2} - \frac{1}{\lambda_c^2}}} \tag{4}$$

$$\varepsilon_r = \frac{{\lambda_0}^2}{\mu_r\left(\frac{1}{\lambda_c^2} - \frac{1}{\Lambda^2}\right)} \tag{5}$$

where $\frac{1}{\Lambda^2}$ is calculated by the eq 6

https://doi.org/10.1021/acsomega.5c02680
ACS Omega 2025, 10, 26041−26051

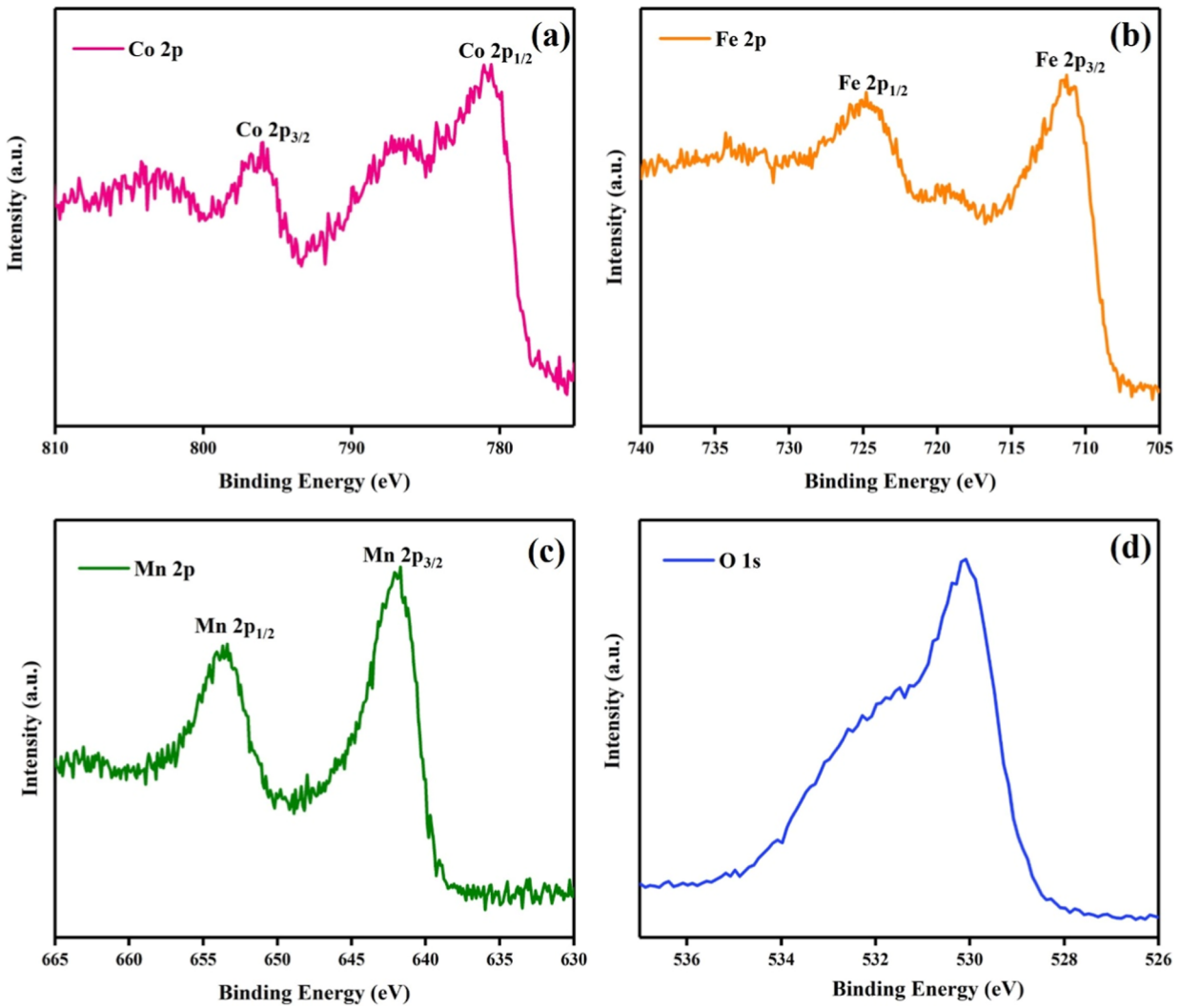

Figure 4. XPS spectra of Co 2p (a), Fe 2p (b), Mn 2p (c) and O 1s (d) for Mn doped $CoFe_2O_4$.

$$\frac{1}{\Lambda^2} = -\left(\left[\frac{1}{2\pi L}\ln\left(\frac{1}{T}\right)\right]\right)^2 \quad (6)$$

where: λ_0 is the free space wavelength, λ_c is the cutoff wavelength of the transmission line section, L is the length of the sample, Λ is a related constant for the measurement.

A key consideration in these measurements is that quarter-wavelength samples are typically used at the frequency of measurement, as the NRW algorithm tends to diverge at frequencies corresponding to multiples of half the sample's wavelength. This ensures accurate results, especially at high frequencies where the material's electromagnetic properties are most relevant for practical applications. This method provides a reliable and efficient way to determine the material's electromagnetic characteristics, including its complex permittivity and permeability, which are essential for evaluating the material's performance in antenna and other magneto-dielectric applications.[20,45]

Figure 5 shows the complex permittivity and permeability measured for Mn doped $Co_2Fe_2O_4$ MDL material. Its evident from the result that the material possess both magnetic electric properties. The permeability of the Mn doped $Co_2Fe_2O_4$ MDL material has a μ'' and μ' vales are around 1.5 and 0.25 in the band. Ther permittivity and permeabilty are near constant across the frequency and also the imaginary parts (ε' and μ') are negligible. The zinc substituted nickel ferrite materials has as permittivity value (ε'') around 2.2 and permeability value (μ'') round 2.2 over the frequency band off 0.5−2.0 GHz.[38] The $NiMn_xFe_{2-x}O_4$ with 0.4 level Mn-substitution has permittivity value (ε'') of 3.8 and permeability value (μ'') of 2.5.[46]

4. ANTENNA DESIGN AND CHARACTERIZATION

4.1. Antenna without Superstrate. A monopole microstrip antenna was designed to operate in the 3.2 GHz−3.6 GHz frequency range for 5G sub-6 GHz applications, such as smartphones and tablets. The antenna uses a microstrip feed line on an FR-4 substrate with a thickness of 1.6 mm. Copper conductors, with a thickness of 52 μm, form the ground plane and antenna. The layout and dimensions of the antenna are shown in Figure 6, and the design was simulated using ADS software. The simulation results confirm that the antenna achieves the desired impedance bandwidth.[47,48]

The fabricated antenna, designed for a center frequency of 3.4 GHz, is shown in Figure 7. The antenna's performance was validated using a Keysight Vector Network Analyzer (N9923A-4 GHz). The simulated and measured return loss results, shown in Figure 5, indicate good agreement, demonstrating

https://doi.org/10.1021/acsomega.5c02680
ACS Omega 2025, 10, 26041−26051

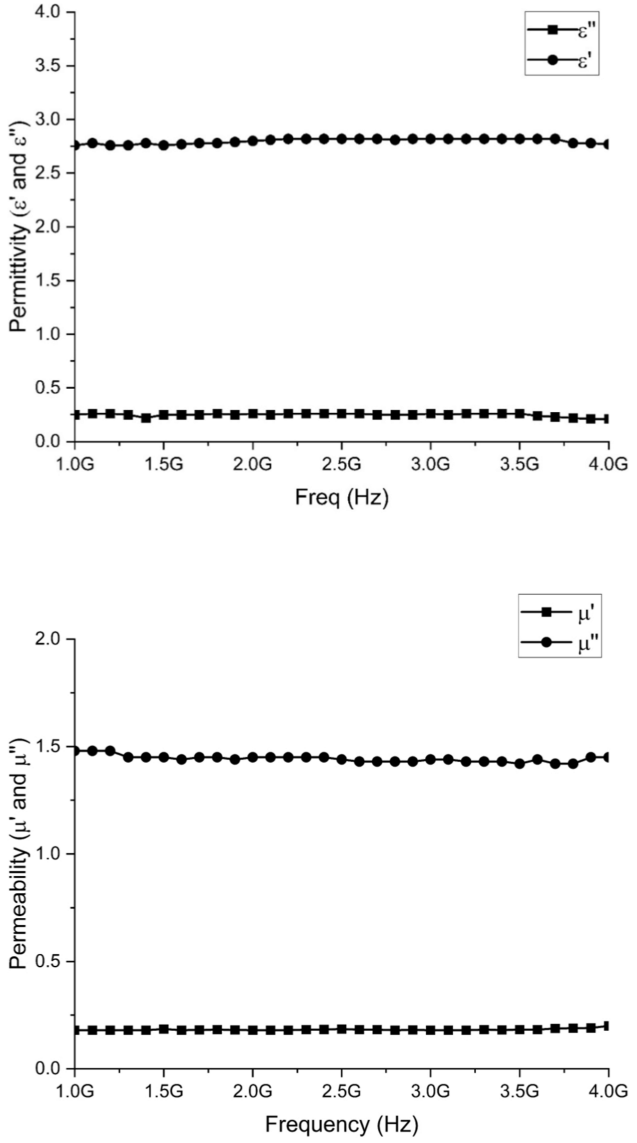

Figure 5. Measured permittivity and permeabiltiy of $Co_{0.6}Mn_{0.4}Fe_2O_4$.

that the antenna effectively covers the 3.2−3.6 GHz frequency range for 5G applications.[16,49]

4.2. Magneto-Dielectric Superstrate Coating. The antenna was coated with a magneto-dielectric material consisting of $CoFe_2O_4$, $Co_{0.6}Mn_{0.4}Fe_2O_4$, and $MnFe_2O_4$, combined with PVDF (polyvinylidene difluoride) and NMP (*N*-methyl-2-pyrrolidone) as solvents. The coating process involved mixing 200 mg of $CoFe_2O_4$, 20 mg of PVDF, and a few drops of NMP. The coating was applied using the doctor blade method and dried after heating, as detailed in previous work on $MnFe_2O4$ and Mn-doped $CoFe_2O_4$ coatings.[50,51] The magneto dielectric material is coated with a thickness of 0.02 mm.

The cross-sectional view of the antenna with the magneto-dielectric superstrate and the antenna with the coating is shown in Figure 8. The performance of the coated antenna was analyzed by measuring its return loss and radiation pattern.

4.3. Return Loss and Performance with Magneto-Dielectric Superstrate. The return loss for antennas with magneto-dielectric coatings was measured and presented in Figure 9. The uncoated antenna resonates at 3.4 GHz, while the superstrate coatings cause shifts in the resonant frequency: $CoFe_2O_4$ shifts it to 3.15 GHz, $Co_{0.6}Mn_{0.4}Fe_2O_4$ shifts it to 3.18 GHz, and $MnFe_2O_4$ shows no shift. The results indicate that $CoFe_2O_4$ and $Co_{0.6}Mn_{0.4}Fe_2O_4$ lower the resonant frequency by 250 and 220 MHz, respectively, implying miniaturization due to increased electrical length.[52]

The uncoated antenna has an impedance bandwidth of 360 MHz, while the superstrate coatings affect this bandwidth. $MnFe_2O_4$ reduces the bandwidth, $CoFe_2O_4$ provides a bandwidth of 352 MHz, and $Co_{0.6}Mn_{0.4}Fe_2O_4$ provides an enhanced bandwidth of 400 MHz. Among all superstrates, $Co_{0.6}Mn_{0.4}Fe_2O_4$ offers the best performance, with improved bandwidth and miniaturization. Multiple layers of coating are applied to the antenna, and its return loss is checked. The results are not enhanced by the numerous coating layers.

4.4. Radiation Pattern and Gain. The radiation patterns of the antenna with and without the superstrate coatings were measured in an anechoic chamber, as shown in Figure 10. The results demonstrate that the coating does not affect the antenna's radiation pattern or efficiency, and the radiation is near omnidirectional in both azimuth and elevation planes.

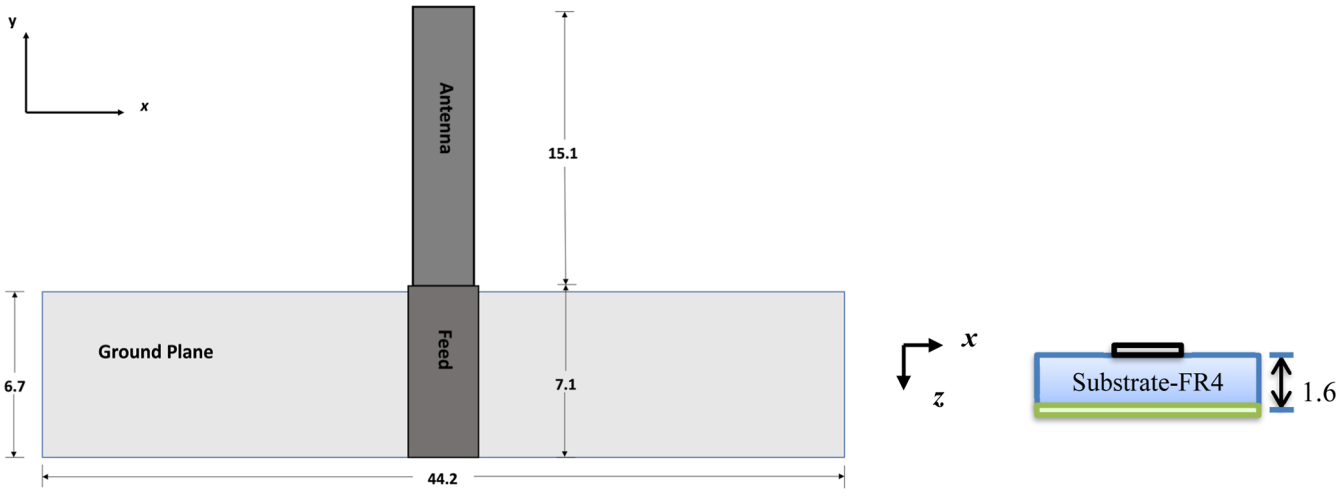

Figure 6. Layout of monopole antenna with dimensions (in mm) before magneto-dielectric coating.

https://doi.org/10.1021/acsomega.5c02680
ACS Omega 2025, 10, 26041−26051

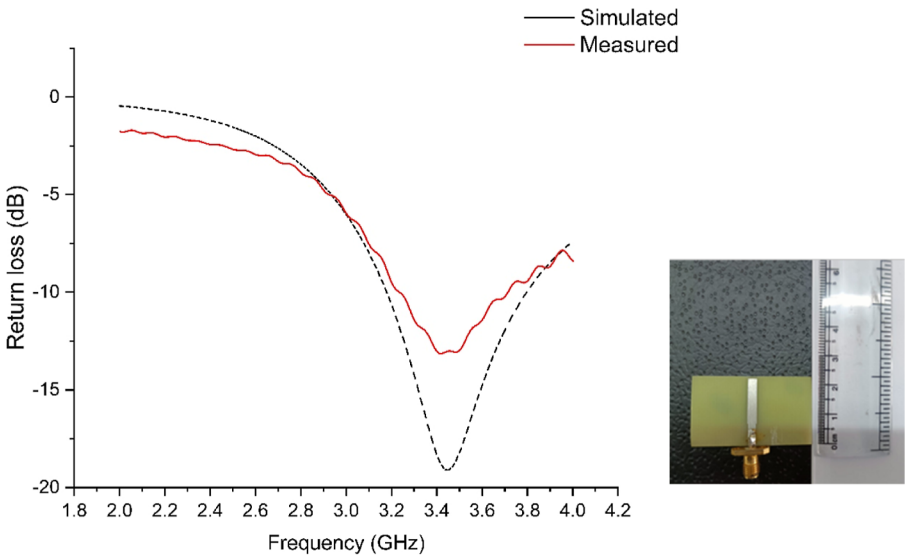

Figure 7. Return loss of simulated and measured results of prototype antenna.

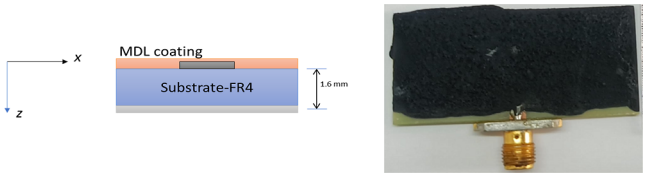

Figure 8. Cross sectional view of antenna with magneto-dielectric (MDL) coating and antenna with magneto-dielectric (MDL) coating.

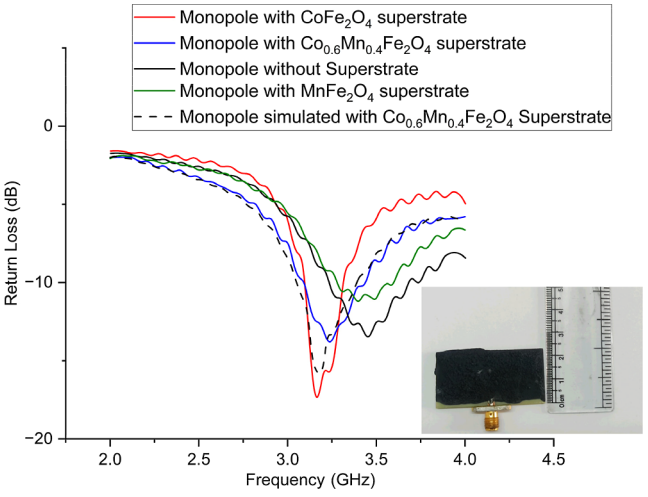

Figure 9. Measured return loss of monopole antenna with and without magneto-dielectric superstrates.

This makes the antenna suitable for hand-held devices operating in the sub-6 GHz band, especially at 3.2−3.4 GHz.

The peak gain of the antenna with superstrate coatings is shown in Figure 11. The antenna with the $MnFe_2O_4$ superstrate provides a peak gain of 2.19 dBi, while the antenna with $CoFe_2O_4$ offers 2.6 dBi, and the $Co_{0.6}Mn_{0.4}Fe_2O_4$ superstrate antenna provides 2.4 dBi. Due to the material's dielectric and magnetic losses, the coating of the magneto-dielectric material has caused a slight decrease in gain values when compared to the traditional printed monopole. However, the significant increase in bandwidth may be advantageous for 5G applications.Thus, the $Co_{0.6}Mn_{0.4}Fe_2O_4$ superstrate delivers the best performance, with a larger bandwidth, better gain, and a reduction in the antenna size by 12%.[53,54]

4.5. Comparison of Magneto-Dielectric Materials.

Table 1 presents a comparison of various magneto-dielectric materials that have been explored for use as substrates or superstrates in antenna designs. These materials play a critical role in enhancing antenna performance by improving factors such as bandwidth, miniaturization, and resonant frequency tuning. Among the materials listed in the table, Mn-doped $CoFe_2O_4$ stands out as the most promising candidate for improving antenna performance, especially for 5G applications in the sub-6 GHz frequency range, which includes the n77 and n78 frequency bands.

4.5.1. Magneto-Dielectric Materials and Their Performance.

- $NiMn_xFe_{2-x}O_4$ Nano Composite: This material, with a frequency band of 722 MHz, provides a relatively narrow bandwidth of 90 MHz. However, it offers a 15% miniaturization of the antenna size. This material is beneficial when there are space constraints, but its limited bandwidth makes it less suitable for high-performance applications like 5G, which require broader frequency coverage for faster data rates.[55]
- $BaLa_xFe_{12-x}O_{19}$: This material operates within the frequency band of 2149 MHz and provides a bandwidth of 166 MHz. Although it offers a reasonably good bandwidth, there is no available data regarding its miniaturization performance. The lack of miniaturization details makes it difficult to assess its suitability for compact devices like smartphones and other portable electronics. Furthermore, the bandwidth is still smaller compared to other materials like Mn-doped $CoFe_2O_4$.[60]
- $Ni_{1-x}Zn_xFe_2O_4$: This material operates at 1500 MHz and provides a bandwidth of 100 MHz. It offers the highest miniaturization performance among the materials listed, at 20%, meaning it can effectively reduce the physical size of antennas. However, its relatively low bandwidth limits its use in applications that require wideband coverage, such as 5G systems, where larger bandwidths are necessary to accommodate high-speed communication.[56]

https://doi.org/10.1021/acsomega.5c02680
ACS Omega 2025, 10, 26041−26051

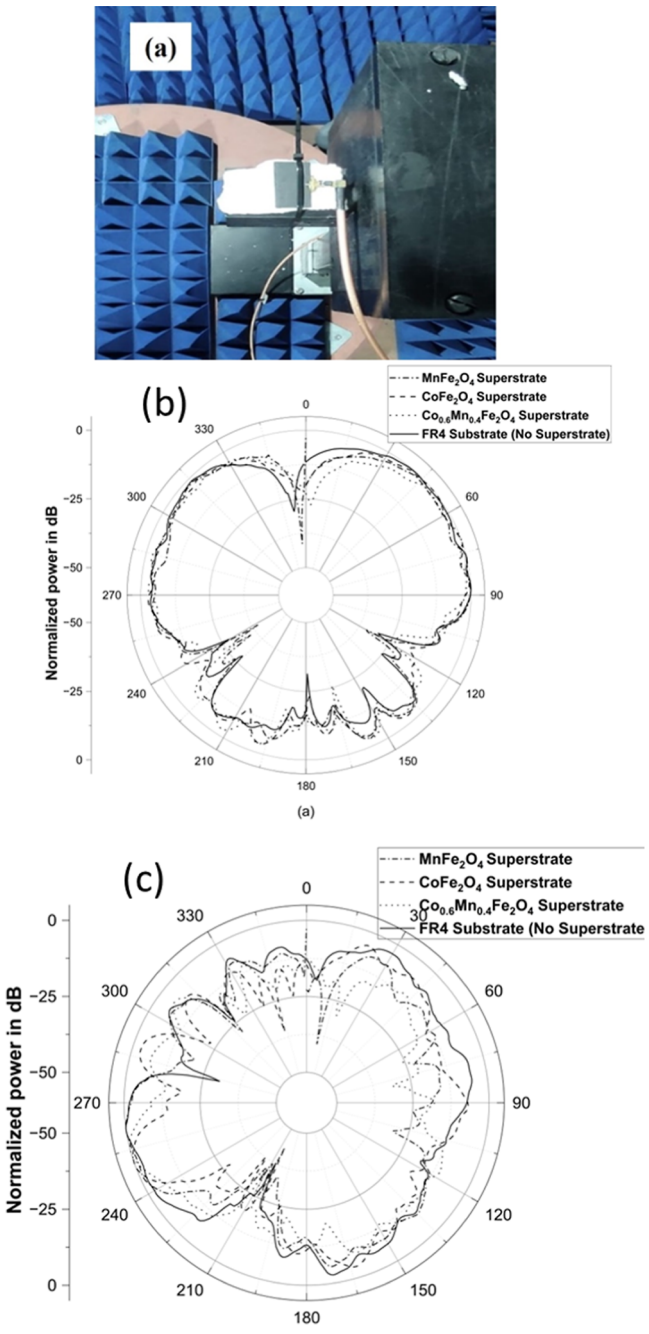

Figure 10. Anechoic chamber (a), radiation pattern with and without magnetic dielectric coating azimuth (b) and elevation (c) plane.

- $Ni_{0.5}Zn_{0.3}Co_{0.2}Fe_2O_4$: This material, operating at 900 MHz, offers a 150 MHz bandwidth but lacks data on its miniaturization performance. While it offers a reasonable bandwidth, the absence of miniaturization information means it cannot be fully evaluated for applications where compactness is essential, such as in hand-held devices or wearable technology.[57,58]

4.5.2. Mn-Doped $CoFe_2O_4$ (Proposed Material). The Mn-doped $CoFe_2O_4$ material, proposed in this study, operates at a frequency band of 3300 MHz, which is highly relevant for 5G sub-6 GHz bands like n77 and n78. This material provides an impressive bandwidth of 400 MHz, which is significantly larger than the other materials, making it highly suitable for high-speed, wideband communication systems. Bandwidth is crucial

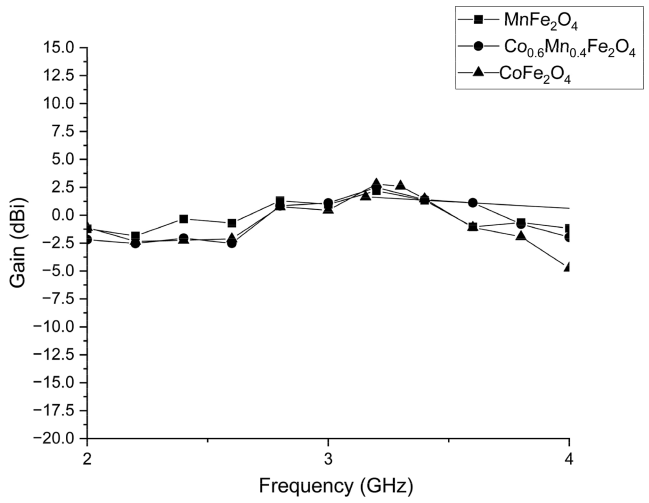

Figure 11. Gain plot of antenna with superstrate coating.

Table 1. Comparison of Performance of Magneto Dielectric Material Supported Antenna

magneto-dielectric material	frequency band	bandwidth	miniaturization (%)
$NiMn_xFe_{2-x}O_4$ nano composite[50]	722 MHz	90 MHz	15
$BaLa_xFe_{12-x}O_{19}$[60]	2149 MHz	166 MHz	not available
$Ni_{1-x}Zn_xFe_2O_4$[33]	1500 MHz	100 MHz	20
$Ni_{0.5}Zn_{0.3}Co_{0.2}Fe_2O_4$[61]	900 MHz	150 MHz	not available
Mn-doped $CoFe_2O_4$ (proposed)	3300 MHz	400 MHz	12

for 5G antennas as it enables them to accommodate multiple frequency channels and provide faster data rates. Additionally, Mn-doped $CoFe_2O_4$ offers a 12% miniaturization, which is substantial but not as high as the 20% offered by $Ni_{1-x}Zn_xFe_2O_4$. Nonetheless, the combination of a large bandwidth and moderate miniaturization makes Mn-doped $CoFe_2O_4$ an ideal choice for 5G antennas.[59]

4.5.3. Why Mn-Doped $CoFe_2O_4$ Stands Out? The key advantage of Mn-doped $CoFe_2O_4$ lies in its balance of performance. It offers a large bandwidth that supports high-speed communication, which is crucial for 5G networks, while still enabling size reduction for compact antenna designs. This combination makes it particularly suitable for smartphones and other mobile devices that need efficient, high-performance antennas operating in the sub-6 GHz range. Its ability to tune the resonant frequency and provide a wider bandwidth ensures that it can handle the high data rates and reliable connectivity required by 5G technologies.[3]

The comparison of magneto-dielectric materials clearly shows that Mn-doped $CoFe_2O_4$ offers superior performance in terms of both bandwidth and miniaturization. While materials like $NiMn_xFe_{2-x}O_4$ nano composite and $Ni_{1-x}Zn_xFe_2O_4$ provide good miniaturization, they fall short in bandwidth, making them less suitable for high-frequency 5G applications. On the other hand, Mn-doped $CoFe_2O_4$ provides the optimal balance, making it a strong candidate for use in 5G smartphones operating in the sub-6 GHz frequency range. It offers improved bandwidth, miniaturization, and resonant frequency tuning, which are essential for enhancing antenna performance in modern wireless communication systems.[62]

https://doi.org/10.1021/acsomega.5c02680
ACS Omega 2025, 10, 26041−26051

5. RESULTS AND DISCUSSION

The performance of the antenna with the $CoFe_2O_4$ superstrate shows a significant improvement in its impedance bandwidth. The antenna achieves a −10 dB bandwidth of 400 MHz, spanning from 3.00 to 3.4 GHz. This wide bandwidth indicates that the antenna can effectively cover a substantial portion of the 5G sub-6 GHz frequency band, which is crucial for efficient communication in devices such as smartphones and tablets. The enhanced bandwidth is a result of the $CoFe_2O_4$ superstrate's impact on the antenna's resonant characteristics, making it more adaptable to the required frequency ranges for modern wireless communications.[63−65]

When Mn-doped $CoFe_2O_4$ is used as the superstrate, the antenna's performance is further enhanced. This modification shifts the antenna's resonance frequency to 3.2 GHz, which is a favorable adjustment for the antenna's operation within the desired 5G frequency range. The shift in the resonance frequency by the Mn-doped material indicates a lowering of the resonant frequency, a phenomenon that can be attributed to the material's unique magnetic and dielectric properties, which effectively increase the electrical length of the antenna. This change in the electrical length leads to antenna miniaturization, allowing for more compact designs, which is a significant advantage in mobile devices where space is a constraint. Additionally, the Mn-doped $CoFe_2O_4$ superstrate results in a peak gain of 2.6 dBi, a noticeable improvement in antenna efficiency. The gain is a critical parameter that indicates the antenna's ability to focus and direct electromagnetic energy, improving its performance for signal transmission and reception. A gain of 2.6 dBi is substantial for mobile communication applications, where higher gain is desired for better signal strength and coverage.[2,13,66]

The combination of Mn-doped $CoFe_2O_4$ and polyvinylidene fluoride (PVDF) as a superstrate material provides a synergistic effect that enhances both impedance matching and radiation characteristics of the antenna. The PVDF material, known for its flexibility and stability, works effectively with the Mn-doped $CoFe_2O_4$ to ensure that the antenna maintains excellent impedance matching across the frequency band. This results in minimal signal reflection, which is crucial for efficient energy transfer between the antenna and the rest of the communication system. In summary, the use of Mn-doped $CoFe_2O_4$−PVDF superstrate enhances the antenna's overall performance by improving impedance bandwidth, resonant frequency tuning, miniaturization, and peak gain. These characteristics make the antenna highly suitable for 5G applications, providing both compactness and high performance, which are essential for the next generation of mobile communication systems. The successful integration of these materials offers a promising pathway for designing antennas that meet the stringent requirements of modern wireless technologies, particularly for hand-held devices operating within the sub-6 GHz frequency range.[67,68]

6. CONCLUSION

In this study, the performance of a monopole microstrip antenna designed for 5G sub-6 GHz applications was significantly enhanced through the use of magneto-dielectric superstrates. Specifically, the $CoFe_2O_4$ and Mn-doped $CoFe_2O_4$ superstrates, when coated on the antenna, led to notable improvements in key performance metrics, including impedance bandwidth, resonant frequency, gain, and miniaturization. The antenna with the Mn-doped $CoFe_2O_4$ superstrate achieved a −10 dB bandwidth of 400 MHz, covering a wide range of the required frequency spectrum. The addition of the Mn-doped $CoFe_2O_4$ superstrate shifted the resonance frequency to 3.2 GHz and achieved a peak gain of 2.6 dBi, further demonstrating the material's effectiveness in optimizing the antenna for 5G communications.

The combination of Mn-doped $CoFe_2O_4$ with PVDF provided an ideal balance between electromagnetic characteristics and mechanical properties, ensuring efficient impedance matching, radiation efficiency, and the desired antenna miniaturization. The results underscore the potential of using magneto-dielectric materials in antenna design to meet the growing demands of 5G mobile devices, offering significant benefits in terms of performance and size reduction.

Overall, this work highlights the advantages of integrating magneto-dielectric materials like Mn-doped $CoFe_2O_4$ for enhancing antenna design in next-generation wireless communication systems. These findings suggest that such materials can play a critical role in the development of compact, high-performance antennas that are capable of operating efficiently in the sub-6 GHz bands, which are essential for the future of 5G technologies.

■ ASSOCIATED CONTENT

Data Availability Statement

All data generated or analyzed during this study are included in this article.

■ AUTHOR INFORMATION

Corresponding Author

Venkatesh Dayanidhi − *Department of Electronics and Communication Engineering, PSG Institute of Technology and Applied Research, Coimbatore, Tamilnadu 641062, India;* orcid.org/0000-0002-0663-6996; Email: venkateshdayanidhi@gmail.com

Authors

Thiyagarajan Krishnan − *Department of Electronics and Communication Engineering, PSG College of Technology Peelamedu, Coimbatore, Tamilnadu 641004, India*

Thangaraju Dheivasigamani − *Nano-Crystal Design and Application Lab (n-DAL), Department of Physics, PSG Institute of Technology and Applied Research, Coimbatore 641062 Tamil Nadu, India;* orcid.org/0000-0003-1928-3779

Complete contact information is available at: https://pubs.acs.org/10.1021/acsomega.5c02680

Author Contributions

Conceptualization, D.V., and T.K.; methodology, D.V., and T.D.; software, D.V.; validation, T.K., and T.D.; investigation, D.V., T.K., and T.D.; resources, D.V., T.K., and T.D.; writing, D.V., T.K., and T.D.; supervision, T.K.; All authors reviewed the manuscript.

Notes

The authors declare no competing financial interest.

■ ACKNOWLEDGMENTS

The authors express their gratitude to the Department of Electronics and Communication Engineering, Government

https://doi.org/10.1021/acsomega.5c02680
ACS Omega 2025, 10, 26041−26051

college of Engineering, Bodinayakanur for providing the facility to measure the radiation pattern in their anechoic chamber.

REFERENCES

(1) Jeon, G.; Ahmad, A.; Chehri, A.; Wen, S. Guest Editorial: Unfolding the potential of 5G technologies for future wireless networks. *IET Networks* **2024**.
(2) Hou, R.; Ren, J.; Liu, Y.-T.; Cai, Y.-M.; Wang, J.; Yin, Y. Broadband Magnetoelectric Dipole Filtering Antenna for 5G Application. *IEEE Antennas Wirel. Propag. Lett.* **2023**, *22* (3), 497−501.
(3) Rahman, A.; Yi, Ng M.; Ahmed, A. U.; Alam, T.; Singh, M. J.; Islam, M. T. A compact 5G antenna printed on manganese zinc ferrite substrate material. *IEICE Electron. Express* **2016**, *13* (11), 20160377.
(4) Mishra, S.; Singh, M. Research Challenges and Opportunities in 5G Network. *International Journal of Future Generation Communication and Networking* **2017**, *10* (6), 13−22.
(5) Abubakar, H. S.; Zhao, Z.; Kiani, S. H.; Khan, S.; Ali, T.; Bashir, M. A.; Cengiz, K.; Kamal, M. M. Eight element MIMO antenna for sub 6 GHz 5G cellular devices. *Phys. Scr.* **2024**, *99* (8), 085559.
(6) Salisu, A.; Ullah, A.; Musa, U.; Akinsolu, M. O.; Hussaini, A. S.; Amar, A. S. I. Dual-Band Microstrip Patch Antenna for Millimeter Wave and Sub-6 GHz Bands with High Frequency Ratio for 5G Application. In *2024 International Telecommunications Conference (ITC-Egypt)*: Cairo, Egypt, 2024, pp 631−634..
(7) Pradeep, P.; Raju, A. R.; Sanjana, V.; Sainithin, M.; Rao, S. P. V. S. Design of a Frequency Selective Surface Backed Wideband Sub-6 GHz Band MIMO Antenna with High Isolation for 5G Applications. In *2024 2nd International Conference on Sustainable Computing and Smart Systems (ICSCSS)*: Coimbatore, India, 2024, pp 460−465..
(8) Koziel, S.; Pietrenko-Dabrowska, A.; Golunski, L. Globalized Knowledge-Based, Simulation-Driven Antenna Miniaturization Using Domain-Confined Surrogates and Dimensionality Reduction. *Appl. Sci.* **2023**, *13*, 8144.
(9) Liu, K.; Sun, D.; Su, T.; Zheng, X.; Li, C. Design of Flexible Multi-Band Miniature Antenna Based on Minkowski Fractal Structure and Folding Technique for Miniature Wireless Transmission System. *Electronics* **2023**, *12*, 3059.
(10) Li, W.; Li, D.; Zhou, K.; Fu, Q.; Yuan, X.; Zhu, X. A Survey of Antenna Miniaturization Technology Based on the New Mechanism of Acoustic Excitation. *IEEE Trans. Antennas Propag.* **2023**, *71* (1), 263−274.
(11) Wu, C.; Zhao, L. A Compact Dual-Polarized Magnetoelectric Dipole Antenna and Array with Wide Scanning Angle for 5G Millimeter Wave Applications. In *2023 Cross Strait Radio Science and Wireless Technology Conference (CSRSWTC)*: Guilin, China, 2023, pp 1−2..
(12) Wang, Y.; Wang, T.; Wang, Y.; Chang, H.; Wang, J.; Xi, Q.; Zi, G.; Jia, Z.; Zhao, S.; Huang, D.; et al. Miniaturized Magnetoelectric Antenna for Low Frequency Electromagnetic Wave Communication. In *2023 IEEE SENSORS*: Vienna, Austria, 2023; pp 01−04..
(13) Jabbar, R.; Sabeeh, S. H.; Hameed, A. M. Structural, dielectric and magnetic properties of Mn+2 doped cobalt ferrite nanoparticles. *J. Magn. Magn. Mater.* **2020**, *494*, 165726−165733.
(14) Lei, Y.; Liu, K.; Huo, X.; Yang, Y.; Wang, X.; Ma, Y.; Yin, Q.; Zhang, H.; Li, J. Mn-substituted Co2Z ferrite ceramics with impedance matching for ultra-high frequency miniaturization antennas. *J. Alloys Compd.* **2024**, *980*, 173552−173563.
(15) He, L.; Fan, P.; Li, S.; Hu, Z.; Wang, H.; Wang, F.; Xi, X. Design and preparation of low-loss Ba(CoTi)M-spinel hybrid ferrites for broadband magnetic-dielectric resonator antenna application. *J. Eur. Ceram. Soc.* **2024**, *44* (13), 7651−7659.
(16) He, Z.; Wang, C.; Sun, R.; Liu, S.; Ding, L.; Gao, T.; Liu, P. Hollow engineering of HCNs@ CoFe 2 Se 4-QDs with quantum dots toward ultra-broadband electromagnetic wave absorption. *J. Adv. Ceram.* **2025**, *14* (4), 9221058.
(17) Zhao, J.; Wang, Z.; Wang, H.; Liu, P.; Che, R. Controllable design of "nested doll" MoS2/V2O3 heterostructures promotes polarization effects for high-efficiency microwave absorption. *Adv. Funct. Mater.* **2025**, *35* (14), 2418282.
(18) Liu, P.; Gao, S.; Liu, X.; Huang, Y.; He, W.; Li, Y. Rational construction of hierarchical hollow CuS@CoS2 nanoboxes with heterogeneous interfaces for high-efficiency microwave absorption materials. *Composites, Part B* **2020**, *192*, 107992.
(19) Liu, P.; Gao, S.; Wang, Y.; Zhou, F.; Huang, Y.; Luo, J. Metal-organic polymer coordination materials derived Co/N-doped porous carbon composites for frequency-selective microwave absorption. *Composites, Part B* **2020**, *202*, 108406.
(20) Thomas, A. M.; Chapman, D. N.; Rogers, C. D. F.; Metje, N.; Atkins, P. R.; Lim, H. M. Broadband Apparent Permittivity Measurement in Dispersive Soils Using Quarter-Wavelength Analysis. *Soil Sci. Soc. Am. J.* **2008**, *72*, 1401−1409.
(21) Asif, R. M.; Aziz, A.; Akhtar, M. N.; Khan, M. A.; Abbasi, M. N.; Abdul Muqeet, H. Synthesis and characterization of cerium doped Ni Zn nano ferrites as substrate material for multi band MIMO antenna. *PLoS One* **2024**, *19* (7), No. e0305060.
(22) Liu, S. Y.; Lin, Z. F.; Chui, S. T. Controlling Electromagnetic Wave Based on Magnetic Metamaterials. *Adv. Sci. Technol.* **2012**, *77*, 237−245.
(23) Parke, L. Controlling the Electromagnetic Properties of Magnetic Composites and Metamaterials. Doctoral Thesis, University of Exeter, United Kingdom, 2015.
(24) Zheng, Z. Flexible High Magnetodielectric Materials for Antenna Applications (Invited). In *2018 International Conference on Microwave and Millimeter Wave Technology (ICMMT)*: Chengdu, China, 2018, pp 1−3..
(25) Chang, P.; He, L.; Wang, H. Low Loss Magneto-Dielectric Composite Ceramics $Ba_3Co_2Fe_{24}O_{41}/SrTiO_3$ for High-Frequency Applications. *J. Am. Ceram. Soc.* **2015**, *98*, 1137−1141.
(26) Su, H.; Tang, X.; Zhang, H.; Jing, Y.; Bai, F. Low-Loss Magneto-Dielectric Materials: Approaches and Developments. *J. Electron. Mater.* **2014**, *43*, 299−307.
(27) Mihalik, M.; Mihalik, M.; Zentková, M.; Uhlířová, K.; Kratochvílová, M.; Roupcová, P. Magneto-crystalline anisotropy of NdFe0.9Mn0.1O3 single crystal. *Phys. B* **2018**, *536*, 89−92.
(28) Jalili, H.; Aslibeiki, B.; Ghotbi Varzaneh, A.; Chernenko, V. A. The effect of magneto-crystalline anisotropy on the properties of hard and soft magnetic ferrite nanoparticles. *Beilstein J. Nanotechnol.* **2019**, *10*, 1348−1359.
(29) Lavorato, G.; Alzamora, M.; Contreras, C.; Burlandy, G.; Litterst, F. J.; Baggio-Saitovitch, E. Internal Structure and Magnetic Properties in Cobalt Ferrite Nanoparticles: Influence of the Synthesis Method. *Part. Part. Syst. Charact.* **2019**, *36*, 190006.
(30) Liu, J.; Römer, I.; Tang, S. V. Y.; Valsami-Jones, E.; Palmer, R. E. Crystallinity depends on choice of iron salt precursor in the continuous hydrothermal synthesis of Fe−Co oxide nanoparticles. *RSC Adv.* **2017**, *7*, 37436−37440.
(31) Gomes, P.; Costa, B.; Carvalho, J. P. F.; Soares, P. I. P.; Vieira, T.; Henriques, C.; Valente, M. A.; Teixeira, S. S. Cobalt Ferrite Synthesized Using a Biogenic Sol−Gel Method for Biomedical Applications. *Molecules* **2023**, *28*, 7737.
(32) Jiang, L.; Yang, S.; Zheng, M.; Wu, A.; Chen, H. Synthesis of polycrystalline CoFe2O4 and NiFe2O4 powders by auto-combustion method using a novel amino-based gel. *Mater. Res. Express* **2017**, *4* (12), 126102.
(33) Khelfallah, M.; Carvallo, C.; Dupuis, V.; Neveu, S.; Taverna, D.; Guyodo, Y.; Guigner, J.-M.; Bertuit, E.; Michot, L.; Baaziz, W.; Ersen, O.; Andersen, I. M.; Snoeck, E.; Gatel, C.; Juhin, A. Structural and Magnetic Properties of Ferrofluids Composed of Self-Assembled Cobalt Ferrite Nanoflowers: A Multiscale Investigation. *J. Phys. Chem. C* **2024**, *128* (31), 13162−13176.
(34) Khan, U.; Nairan, A.; Naz, S.; Wang, X.; Khan, K.; Tareen, A. K.; Wu, D.; Gao, J. Optical and temperature-dependent magnetic properties of Mn-doped CoFe2O4 nanostructures. *Mater. Today Commun.* **2023**, *35*, 106276.

https://doi.org/10.1021/acsomega.5c02680
ACS Omega 2025, 10, 26041−26051

(35) Ansari, S. M.; Phase, D.; Kolekar, Y. D.; Ramana, C. V. Effect of Manganese-Doping on the chemical and optical properties of cobalt ferrite nanoparticles. *J. Mater. Sci. Eng. B* **2024**, *300*, 117134.
(36) Rady, K. E.; Reda Abd El-salam, A.; Elfadaly, E. A.; Aly, M. H. Effect of Mn2+ Substitution on Structural and Magnetic Properties of Co-Zn Ferrite. *ECS J. Solid State Sci. Technol.* **2023**, *12*, 113003.
(37) Milutinović, A.; Lazarević, Z. Ž.; Šuljagić, M.; Andjelković, L. Synthesis-Dependent Structural and Magnetic Properties of Monodomain Cobalt Ferrite Nanoparticles. *Metals* **2024**, *14*, 833.
(38) Deepak Ram Prasath, S.; Balaji, S.; Raju, S.; Abhaikumar, V. Synthesis and characterization of zinc substituted nickel ferrite materials for L band antenna applications. *J. Mater. Sci.: Mater. Electron.* **2016**, *27*, 8247−8253.
(39) Apostolova, I. N.; Apostolov, A. T.; Wesselinowa, J. M. M. Band Gap and Specific Heat of Pure and Ion Doped $MnFe_2O_4$ Nanoparticles. *Magnetochemistry* **2023**, *9* (3), 76.
(40) Zeng, M.; Liu, J.; Yue, M.; Yang, H.; Dong, H.; Tang, W.; Jiang, H.; Liu, X.; Yu, R. High-frequency electromagnetic properties of the manganese ferrite nanoparticles. *J. Appl. Phys.* **2015**, *117* (17), 17B527.
(41) Wang, C.; Liu, X.; Zhang, D.; Zhang, R.; Yang, X.; Wang, Y. A high sensitivity planar electric−magnetic isolated sensor for full characterization of magneto dielectric materials. *Measurement* **2024**, *232*, 114708.
(42) Sorocki, J.; Piekarz, I.; Bozzi, M. Broadband Permittivity and Permeability Extraction of 3-D-Printed Magneto-Dielectric Substrates. *IEEE Microw. Wirel. Compon. Lett.* **2021**, *31* (10), 1174−1177.
(43) Wu, W.-J.; Zhao, W.-S.; Wang, D.-W.; Yuan, B.; Wang, G. A dual-mode microstrip sensor for simultaneously extracting complex permittivity and permeability of magnetodielectric samples. *Sens. Actuators, A* **2023**, *349*, 114000.
(44) Peña Rodríguez, G.; Vera Barrera, R.; Mancipe Huérfano, D. L.; Lara González, L. Á.; Ángel, L. Propiedades electromagnéticas de un compuesto magneto dieléctrico a través de un algoritmo basado en el método Nicolson-Ross-Weir. *Ing. Investig. Desarr.* **2021**, *21* (1), 59−69.
(45) Shan, J.; Ke, X. Measurement of the Electromagnetic Properties of Materials Based on A Refined Transmission-Reflection Algorithm. In *2007 International Symposium on Electromagnetic Compatibility*: Qingdao, China, 2007, pp 178−181..
(46) Jude, A.; Balaji, S.; Prasath, S. D. R.; Raju, S.; Abhaikumar, V. Miniaturization of long-term evolution antenna fostered by NiMnxFe2−xO4 nano composite coating. *Mater. Res. Express* **2019**, *6* (9), 96307.
(47) Pradeep, P.; Kottareddygari, J. S.; Sekhar, P. C. Design of a Novel Compact L-slotted Monopole Antenna for 5G Applications in sub-6 GHz Band. In *2022 3rd International Conference on Electronics and Sustainable Communication Systems*; ICESC): Coimbatore, India, 2022, pp 394−397..
(48) Verma, R. K.; Priya, B.; Singh, M.; Singh, P.; Yadav, A.; Singh, V. K. Equivalent circuit model-based design and analysis of microstrip line fed electrically small patch antenna for sub-6 GHz 5G applications. *Int. J. Commun. Syst.* **2023**, *36* (17), 5595.
(49) Tian Teck, C.; Al-Fadhali, N.; Majid, H.; Jumadi, J.; Shairi, A.; M Gisamalla, M. S.; Ashyap, A.; Mukred, J.; Abo Mosali, N. Developing and Verifying A 3.5ghz Smart Antenna for Wideband 5G Communication. *J. Adv. Manuf. Technol.* **2023**, *4* (1), 9−16.
(50) Koutinos, A. G.; Zekios, C. L.; Georgakopoulos, S. V. An HF Magnetoelectric Dipole Element. In *2023 IEEE International Symposium on Antennas and Propagation and; USNC-URSI Radio Science Meeting (USNC-URSI)*: Portland, OR, USA, 2023, pp 1527−1528..
(51) Chevalier, A.; Breiss, H.; Hoez, A.; Mattei, J.-L. Magnetodielectric Material for VHF Antenna Devices Tunable by a Low DC Magnetic Field. *IEEE Trans. Magn.* **2023**, *59* (11), 1−5.
(52) Han, K.; Swaminathan, M.; Pulugurtha, R.; Sharma, H.; Tummala, R.; Nair, V. Magneto-dielectric material characterization and antenna design for RF applications. In *8th European Conference on Antennas and Propagation (EuCAP 2014)*: The Hague, Netherlands, 2014, pp 381−384..
(53) Huang, M. D.; Tan, S. Y. Radiation Characteristics of a Prolate Spheroidal Antenna Coated with a Double-Negative Metamaterial Radome. *Waves in Random and Complex Media* **2009**, *19* (3), 409−417.
(54) Niamien, C.; Collardey, S.; Sharaiha, A.; Mahdjoubi, K.; Mattei, J. L. Ultra-miniature planar UHF antenna using a magneto-dielectric superstrate. In *2010 Loughborough Antennas & Propagation Conference*; Loughborough: UK, 2010, pp 437−440..
(55) Reddaf, A.; Medjili, F.; Faci, Y. Miniaturization of a patch antenna by thin film materials. In *The First National Conference on Electronics and New Technologies (NCENT'2015)*, 2015.
(56) Chevalier, A.; Le Guen, E.; Tarot, A.-C.; Grisart, B.; Souriou, D.; Thakur, A.; Queffelec, P.; Mattei, J.-L. Influence de ferrites de Ni-Zn dans la miniaturisation d'antennes pour applications DVB-H. In *17èmes Journées Nationales Microondes*: Brest, France, 2011..
(57) Saini, A.; Thakur, A.; Thakur, P. Matching permeability and permittivity of $Ni_{0.5}Zn_{0.3}Co_{0.2}In_{0.1}Fe_{1.9}O_4$ ferrite for substrate of large bandwidth miniaturized antenna. *J. Mater. Sci.: Mater. Electron.* **2016**, *27*, 2816−2823.
(58) Mattei, J.-L.; Le Guen, E.; Chevalier, A. Dense and half-dense NiZnCo ferrite ceramics: Their respective relevance for antenna downsizing, according to their dielectric and magnetic properties at microwave frequencies. *J. Appl. Phys.* **2015**, *117* (8), 084904.
(59) Yunasfi, Y.; Mashadi, M.; Winatapura, D. S.; Setiawan, J.; Taryana, Y.; Gunanto, Y. E.; Adi, W. A. Enhanced Magnetic and Microwave Absorbing Properties of Nd^{3+} Ion Doped $CoFe_2O_4$ by Solid-State Reaction Method. *Phys. Status Solidi A* **2023**, *220*, 2200718.
(60) Gokulnath, C.; Balaji, S.; Deepak Ram Prasath, S.; Raju, S.; Abhaikumar, V. An investigation of $BaLa_xFe_{12-x}O_{19}$ magneto dielectric material to develop miniaturized antenna for navigational applications. *Mater. Res. Express* **2018**, *5* (7), 076103.
(61) Zheng, Z.; Wu, X. A Miniaturized UHF Vivaldi Antenna With Tailored Radiation Performance Based on Magneto-Dielectric Ferrite Materials. *IEEE Trans. Magn.* **2020**, *56* (3), 1−5.
(62) Ahsan, M. Z.; Khan, F. A.; Islam, M. A. Frequency and Temperature Dependent Dielectric and Magnetic Properties of Manganese Doped Cobalt Ferrite Nanoparticles. *J. Electron. Mater.* **2019**, *48*, 7721−7729.
(63) Rajalakshmi, B.; Prathicksha, S.; Harsha, K.; Varshini, M. A.; Anisha, T. A Broadband MIMO Antenna for 5G Application. In *2024 International Conference on Communication; Computing and Internet of Things (IC3IoT)*: Chennai, India, 2024, pp 1−6..
(64) Zhou, M.; Xu, Y.; Wang, A.; Hou, J. A wideband magnetoelectric dipole antenna for 4G/5G communication. *Microw. Opt. Technol. Lett.* **2023**, *65*, 2941−2946.
(65) Chen, P.; Feng, Y.; Shen, W.; Li, H.; Li, G. Improvement of the Bandwidth and Gain of an Antenna Based on a Ferrite Material by Using a Metamaterial Superstrate. In *2020 International Conference on Microwave and Millimeter Wave Technology (ICMMT)*: Shanghai, China, 2020, pp 1−3..
(66) Adhiyoga, Y. G.; Rahman, S. F.; Apriono, C.; Rahardjo, E. T. Miniaturized 5G Antenna With Enhanced Gain by Using Stacked Structure of Split-Ring Resonator Array and Magneto-Dielectric Composite Material. *IEEE Access* **2022**, *10*, 35876−35887.
(67) Gonçalves, R.; Martins, P.; Moya, X.; Ghidini, M.; Sencadas, V.; Gabriela, B.; Mathur, N. D.; Lanceros-Méndez, S. Magnetoelectric CoFe2O4 /polyvinylidene fluoride electrospun nanofibres. *Nanoscale* **2015**, *7*, 8058−8061.
(68) Hussein, M. M.; Saafan, S. A.; Abosheiasha, H. F.; Zhou, D.; Tishkevich, D. I.; Abmiotka, N. V.; Trukhanova, E. L.; Trukhanov, A. V.; Trukhanov, S. V.; Hossain, M. K.; Darwish, M. A. Preparation, structural, magnetic, and AC electrical properties of synthesized CoFe2O4 nanoparticles and its PVDF composites. *Mater. Chem. Phys.* **2024**, *317*, 129041.

https://doi.org/10.1021/acsomega.5c02680
ACS Omega 2025, 10, 26041−26051